Inorganic Chemistry

Article

pubs.acs.org/IC

Design of Pore Size and Functionality in Pillar-Layered Zn-Triazolate-Dicarboxylate Frameworks and Their High CO_2/CH_4 and C2 Hydrocarbons/CH_4 Selectivity

Quan-Guo Zhai,[†,‡] Ni Bai,[‡] Shu'ni Li,[‡] Xianhui Bu,[*,§] and Pingyun Feng[*,†]

[†]Department of Chemistry, University of California, Riverside, California 92521, United States

[‡]School of Chemistry & Chemical Engineering, Shaanxi Normal University, Xi'an, Shaanxi 710062, People's Republic of China

[§]Department of Chemistry and Biochemistry, California State University, Long Beach, California 90840, United States

Supporting Information

ABSTRACT: In the design of new materials, those with rare and exceptional compositional and structural features are often highly valued and sought after. On the other hand, materials with common and more accessible modes can often provide richer and unsurpassed compositional and structural variety that makes them a more suitable platform for systematically probing the composition−structure−property correlation. We focus here on one such class of materials, pillar-layered metal−organic frameworks (MOFs), because different pore size and shape as well as functionality can be controlled and adjusted by using pillars with different geometrical and chemical features. Our approach takes advantage of the readily accessible layered Zn-1,2,4-triazolate motif and diverse dicarboxylate ligands with variable length and functional groups, to prepare seven Zn-triazolate-dicarboxylate pillar-layered MOFs. Six different gases (N_2, H_2, CO_2, C_2H_2, C_2H_4, and CH_4) were used to systematically examine the dependency of gas sorption properties on chemical and geometrical properties of those MOFs as well as their potential applications in gas storage and separation. All of these pillar-layered MOFs show not only remarkable CO_2 uptake capacity, but also high CO_2 over CH_4 and C2 hydrocarbons over CH_4 selectivity. An interesting observation is that the BDC ligand (BDC = benzenedicarboxylate) led to a material with the CO_2 uptake outperforming all other metal-triazolate-dicarboxylate MOFs, even though most of them are decorated with amino groups, generally believed to be a key factor for high CO_2 uptake. Overall, the data show that the exploration of the synergistic effect resulting from combined tuning of functional groups and pore size may be a promising strategy to develop materials with the optimum integration of geometrical and chemical factors for the highest possible gas adsorption capacity and separation performance.

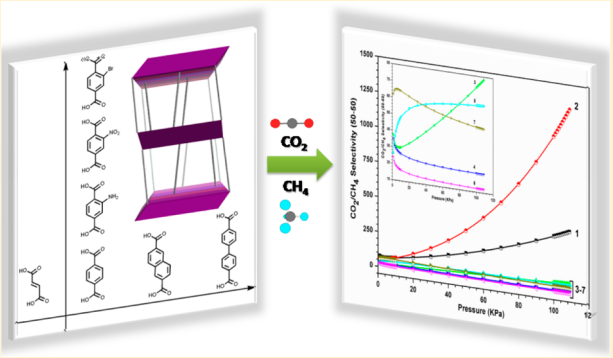

INTRODUCTION

The separation of CO_2 and C2 hydrocarbons from CH_4 is an important process in natural gas upgrading because the high concentrations of CO_2 and C2 hydrocarbons will not only hinder the complete conversion of methane,[1] but also generate the corrosion of gas pipeline.[2] However, up to now, such separation remains a significant challenge,[3] although extensive efforts have been made worldwide to develop efficient and economical separation technology.

In the past decade, porous coordination polymers (PCPs) or metal−organic frameworks (MOFs) have shown promise as cost-effective and efficient materials for adsorption and separation because of their enormous structural variety and controllable pore structures.[4,5] Although a large number of MOFs have been designed by taking advantage of the assemblies of organic linkers and metal or cluster connectors, only a small number of them show outstanding selectivity for CO_2 over CH_4.[3] Furthermore, the separation of C2 hydrocarbons from CH_4 mixtures utilizing MOFs has been much less studied[6] due to their similar physical and chemical properties. Thus, the exploration of MOFs for possible applications in high-capability separation of CH_4 is needed.

To achieve high CO_2 adsorption capacity and separations of CO_2 or C2 hydrocarbons from CH_4, various strategies have been explored in the construction of MOFs, including controlling the pore size/shape,[7] introducing functional groups,[8] generating open metal sites,[9] and forming charged frameworks.[10] Although the investigation on each individual factor on CO_2 uptake and adsorption selectivity of MOFs offers insight into the role each factor plays, it is undoubtedly important to study the synergistic effect of different factors such as the pore size and functional groups because these factors could function cooperatively to enhance the gas uptake and

Received: July 21, 2015
Published: October 2, 2015

DOI: 10.1021/acs.inorgchem.5b01611
Inorg. Chem. 2015, 54, 9862−9868

selectivity. In this light, pillar-layered MOFs are promising because the layer structural motif is usually not affected by the alteration of the pillars, and different pore size and shape as well as functionality may be controlled and adjusted by utilization of different pillars.

One rational method to construct pillared-layer MOF structures is to apply rigid carboxylate ligands to bridge 2D layers formed by metal ions and amines. The rigid carboxylate ligands have a great ability to adopt different bonding modes and satisfy various metal coordination preferences. Among different 2D layer configurations, except the well-known metal−pyridine system, metal-1,2,4-triazolate motifs have attracted significant interest.[11] A number of metal-triazolate-dicarboxylate pillar-layered frameworks have been constructed;[12] however, only a limited number of them exhibited selective CO_2 uptake. For example, Shimizu et al. reported a microporous framework $[Zn_2(atz)_2(ox)]$ showing high CO_2 uptake and adsorption enthalpy.[13] Zhang et al. synthesized three Zn-triazolate-dicarboxylate MOFs with remarkable adsorption capacity and selectivity for CO_2.[14] Wang et al. reported two isomeric MOFs, consisting of Co-triazolate layers and positional isomeric dicarboxylate pillars. Both showed distinct temperature-dependent CO_2 sorption behaviors.[15] However, the selective CO_2 uptakes of above-mentioned pillar-layered MOFs all were ascribed to amino groups in the metal-triazolate layer. Further investigation on pore size and functionality as well as their synergistic effect on CO_2 adsorption and selectivity is undoubtedly significant for the development of target MOFs materials.

Prior to this work, we discovered high CO_2 uptake capacity in a Zn carboxylate 1,2,4-triazolate framework consisting of amino-decorated nanoscopic polyhedral cages,[16] which demonstrated the rich potential of this system in gas sorption applications. In this work, we present a systematic design of pore size and functionality in pillar-layered Zn-triazolate-dicarboxylate MOFs. In our strategy, the (4,4)-layered Zn-1,2,4-triazolate motif is selected to combine with seven rigid ditopic carboxylate ligands with different length and functional groups to form pillar-layered MOFs (Scheme 1). Seven pillar-layered MOFs were successfully synthesized under solvothermal conditions, $[Zn_2(TRZ)_2(L)]$ (TRZ = 1,2,4-triazole, L = fumaric acid, FA for **1**, 1,4-benzenedicarboxylic acid, BDC for **2**, 2-amino-1,4-benzenedicarboxylic acid, NH_2-BDC for **3**, 2-nitro-1,4-benzenedicarboxylic acid, NO_2-BDC for **4**, 2-bromo-1,4-benzenedicarboxylic acid, Br-BDC for **5**, naphthalene-2,6-dicarboxylic acid, NDC for **6**, and 4,4′-biphenyldicarboxylic acid, BPDC for **7**). All of these pillar-layered MOFs show not only remarkable CO_2 uptake capacity, but also high CO_2 over CH_4 and C2 hydrocarbons over CH_4 selectivity. Specially, the CO_2 uptake of compound **2** outperforms all metal-triazolate-dicarboxylate pillar-layered MOFs, even though most of them are decorated with amino groups.[13−15]

Scheme 1. Design of Zn-Triazolate-Dicarboxylate Pillar-Layered Frameworks

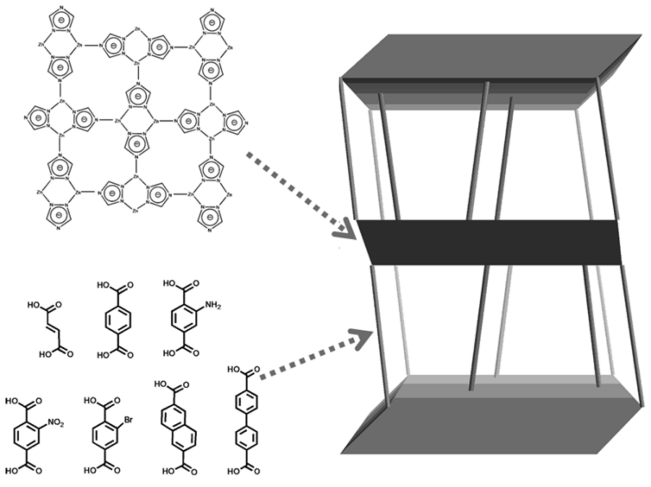

EXPERIMENTAL SECTION

Materials and Methods. $Zn(NO_3)_2{\cdot}6H_2O$, 1,2,4-triazole (TRZ), fumaric acid (FA), 1,4-benzene-dicarboxylic acid (BDC), 2-amino-1,4-benzenedicarboxylic acid (NH_2-BDC), 2-nitro-1,4-benzenedicarboxylic acid (NO_2-BDC), 2-bromo-1,4-benzenedicarboxylic acid (Br-BDC), naphthalene-2,6-dicarboxylic acid (NDC), 4,4′-biphenyldicarboxylic acid (BPDC), *N*,*N*-dimethylformide (DMF), *N*,*N*-dimethylacetamide (DMA), 1,3-dimethyl-2-imidazolidinone (DMI), CH_3CH_2OH, and CH_3OH were purchased from TCI and used as received without further purification. The FT-IR spectra (KBr pellets) were recorded on a Nicolet Avatar 360 FT-IR spectrometer in the range of 4000−400 cm^{-1}. The powder X-ray diffraction patterns (PXRD) were recorded on a Bruker D8 Advance (40 kV, 40 mA) diffractometer (Cu radiation, λ = 1.54056 Å) with a scan speed of 0.5 s/deg at room temperature. Thermal stability studies were carried out on a NETSCHZ STA-449C thermoanalyzer under nitrogen atmosphere (40−1000 °C range) at a heating rate of 5 °C/min.

X-ray Structure Studies. Single-crystal X-ray analysis was performed on a Bruker Smart APEX II CCD area diffractometer with nitrogen-flow temperature controller using graphite-monochromated Mo Kα radiation (λ = 0.71073 Å), operating in the ω and φ scan mode. The SADABS program was used for absorption correction. The structure was solved by direct methods, and the structure refinements were based on $|F|^2$ with anisotropic displacement using SHELXTL.[17] All non-hydrogen atoms in the framework were refined with anisotropic displacement parameters. The large volume fractions of solvents in the lattice pores could not be modeled in terms of atomic sites and were treated using the SQUEEZE routine in the PLATON software package.[18] Crystal data as well as details of data collection and refinements were summarized in Tables S1−S4. CCDC 1062753−1062759 for compounds **1**−**7** contain the supplementary crystallographic data for this Article. These crystal data can be obtained free of charge from The Cambridge Crystallographic Data Centre through www.ccdc.cam.ac.uk/data_request/cif.

Syntheses. *$[Zn_2(TRZ)_2(FA)]$ (**1**).* In a 25 mL glass vial were dissolved 59.5 mg of $Zn(NO_3)_2{\cdot}6H_2O$, 6.9 mg of TRZ, and 11.6 mg of FA in a mixture of 2 mL of DMA, 1 mL of CH_3OH, and 1 mL of H_2O. The vial was sealed and placed in a 90 °C oven for 3 days. Pure block colorless crystals were obtained after cooling to room temperature. The yield was about 82% based on Zn. Pure sample was obtained by filtering and washing the raw product with DMA.

*$[Zn_2(TRZ)_2(BDC)]$ (**2**).* In a 25 mL glass vial were dissolved 297.5 mg of $Zn(NO_3)_2{\cdot}6H_2O$, 34.5 mg of TRZ, and 83.3 mg of BDC in a mixture of 4 mL of DMF and 2 mL of H_2O. The vial was sealed and placed in a 90 °C oven for 5 days. Pure block colorless crystals were obtained after cooling to room temperature. The yield was about 90% based on Zn. Pure sample was obtained by filtering and washing the raw product with DMF.

*$[Zn_2(TRZ)_2(NH_2\text{-}BDC)]$ (**3**).* In a 25 mL glass vial were dissolved 148.8 mg of $Zn(NO_3)_2{\cdot}6H_2O$, 34.5 mg of TRZ, and 45.3 mg of NH_2-BDC in a mixture of 4 mL of DMF and 1 mL of H_2O. The vial was sealed and placed in a 120 °C oven for 5 days. Pure block colorless crystals were obtained after cooling to room temperature. The yield was about 74% based on Zn. Pure sample was obtained by filtering and washing the raw product with DMF.

*$[Zn_2(TRZ)_2(NO_2\text{-}BDC)]$ (**4**).* In a 25 mL glass vial were dissolved 74.4 mg of $Zn(NO_3)_2{\cdot}6H_2O$, 17.5 mg of TRZ, and 52.8 mg of NO_2-BDC in

DOI: 10.1021/acs.inorgchem.5b01611
Inorg. Chem. 2015, 54, 9862−9868

a mixture of 3 mL of DMA, 1 mL of DMI, and 1 mL of H_2O. The vial was sealed and placed in a 100 °C oven for 3 days. Pure block light yellow crystals were obtained after cooling to room temperature. The yield was about 65% based on Zn. Pure sample was obtained by filtering and washing the raw product with DMA.

[Zn_2(TRZ)$_2$(Br-BDC)] (**5**). In a 25 mL glass vial were dissolved 59.5 mg of $Zn(NO_3)_2{\cdot}6H_2O$, 13.8 mg of TRZ, and 24.5 mg of Br-BDC in a mixture of 2 mL of DMF and 1 mL of H_2O. The vial was sealed and placed in a 90 °C oven for 2 days. Pure block colorless crystals were obtained after cooling to room temperature. The yield was about 75% based on Zn. Pure sample was obtained by filtering and washing the raw product with DMF.

[Zn_2(TRZ)$_2$(NDC)] (**6**). In a 25 mL glass vial were dissolved 89.3 mg of $Zn(NO_3)_2{\cdot}6H_2O$, 20.7 mg of TRZ, and 64.9 mg of NDC in a mixture of 2 mL of DMA, 2 mL of CH_3OH, and 2 mL of H_2O. The vial was sealed and placed in a 90 °C oven for 4 days. Pure block colorless crystals were obtained after cooling to room temperature. The yield was about 58% based on Zn. Pure sample was obtained by filtering and washing the raw product with DMF.

[Zn_2(TRZ)$_2$(BPDC)] (**7**). In a 25 mL glass vial were dissolved 89.3 mg of $Zn(NO_3)_2{\cdot}6H_2O$, 20.7 mg of TRZ, and 73.3 mg of BPDC in a mixture of 3 mL of DMA, 3 mL of CH_3CH_2OH, and 1.5 mL of H_2O. The vial was sealed and placed in a 90 °C oven for 3 days. Pure colorless sheet crystals were obtained after cooling to room temperature. The yield was about 72% based on Zn. Pure sample was obtained by filtering and washing the raw product with DMA.

Gas Adsorption. Gas sorption isotherms were measured on a Micromeritics ASAP 2020HD88 surface-area and pore-size analyzer up to 1 atm of gas pressure by the static volumetric method. As-synthesized samples were activated at 80 °C (**1**, **3**, **6**, and **7**) or 120 °C (**2**, **4**, and **5**) for 12 h. All gases used were of 99.99% purity, and the impurity trace water was removed by passing the gases through the molecular sieve column equipped in the gas line. The gas sorption isotherms for N_2 and H_2 were measured at 77 K. The gas sorption isotherms for CO_2, CH_4, C_2H_2, and C_2H_4 were measured at 273 or 298 K.

Selectivity Prediction for Binary Mixture Adsorption. Ideal adsorbed solution theory (IAST)[19,20] was used to predict binary mixture adsorption from the experimental pure-gas isotherms. To perform the integrations required by IAST, the single-component isotherms should be fitted by a proper model. There is no restriction on the choice of the model to fit the adsorption isotherms; however, data over the pressure range under study should be fitted precisely.[21,22] Several isotherm models were tested to fit the experimental pure isotherms for CH_4, C_2H_4, C_2H_2, and CO_2, and the dual-site Langmuir–Freundlich equation was found to be the best fit to the experimental data:

$$q = q_{m1}[b_1P^{1/n1}/(1 + b_1P^{1/n1})] + q^{m2}[b_2P^{1/n2}/(1 + b_2P^{1/n2})]$$

Here, P is the pressure of the bulk gas at equilibrium with the adsorbed phase (kPa), q is the adsorbed amount per mass of adsorbent (mol/kg), q_{m1} and q_{m2} are the saturation capacities of sites 1 and 2 (mol/kg), b_1 and b_2 are the affinity coefficients of the sites (1/kPa), and n_1 and n_2 are measures of the deviations from an ideal homogeneous surface. The R_2 values for all of the fitted isotherms were over 0.99. Hence, the fitted isotherm parameters were applied to perform the necessary integrations in IAST.

RESULTS AND DISCUSSION

Synthesis. By varying reaction temperatures from 90 to 120 °C and compositions of binary and ternary solvents, solvothermal reactions of $Zn(NO_3){\cdot}6H_2O$, TRZ, and carboxylate ligands afforded pure crystals of compounds **1**–**7**. All exhibit isoreticular pillared-layer structures containing Zn-triazolate layers and dicarboxylate pillars. The powder X-ray diffraction patterns of compounds **1**–**7** are consistent with the simulated ones from single-crystal structures, indicating the phase purity of the as-synthesized samples (Figure S1). FT-IR spectra display the characteristic absorption band for the main functional groups of complexes **1**–**7** (Figure S2). The bands in the 3000–3500 and 1100–1300 cm^{-1} regions are related to ν(C–H) and ν(C–N) or ν(N–N) of the TRZ ligand. The absorption bands in the range of 1350–1650 cm^{-1} are assigned to the ν_{as}(C–O) and ν_{sym}(C–O) of carboxylate groups.

Crystal Structure. Single-crystal X-ray crystallography study shows that MOFs **1**–**5** and **7** crystallize in the tetragonal *P*4/*ncc* space group (Tables S1–S4) with the asymmetric unit containing one Zn^{2+} ion, one TRZ, and half ditopic carboxylate ligands. On the other hand, **6** is in the orthorhombic $Pna2_1$ space group (Table S3), and four unique Zn^{2+}, four TRZ, and two NDC ligands exist in the asymmetric unit. The Zn centers are all 4-coordinated to one carboylate oxygen atom and three nitrogen atoms from three separate triazolate ligands (Figure S3). Each TRZ ligand binds to three Zn ions through typical $\mu_{1,2,4}$-bridging fashion, which leads to a two-dimensional Zn-triazolate layer showing 4.8^2 topology similar to that found in copper(I) and silver(I) triazolates.[23]

Notably, the 2D Zn-TRZ layer is not planar but corrugated due to the existence of tetrahedrally coordinated Zn centers. These 2D layer motifs are further connected by linear dicarboxylate pillars via the Zn–O coordinated bonds to generate the 3D pillar-layered structures of **1**–**7** (Figures S4 and S5). The distances between two adjacent layers vary with the length of pillars, ranging from about 8.8 Å for **1**, 10.8 Å for **2**–**5**, 12.9 Å for **6**, to 15.1 Å for **7**. Topologically, ditopic carboxylate ligands can be viewed as linkers. The tetrahedrally coordinated Zn(II) and tridentate TRZ ligand can be simplified as 4- and 3-connected nodes, producing a (3,4)-connected self-penetrated net with $\{4{\cdot}6{\cdot}8\}\{4{\cdot}6^2{\cdot}8^3\}$ point symbol (Figure S6). Alternatively, if $Zn_2(TRZ)_2$ dimers are regarded as nodes, these pillar-layered MOFs can be represented by a 6-connected *pcu* network consisting of the corresponding $\{[Zn_2(TRZ)_2]_8(L)_4\}$ super building blocks as shown in Figure 1.

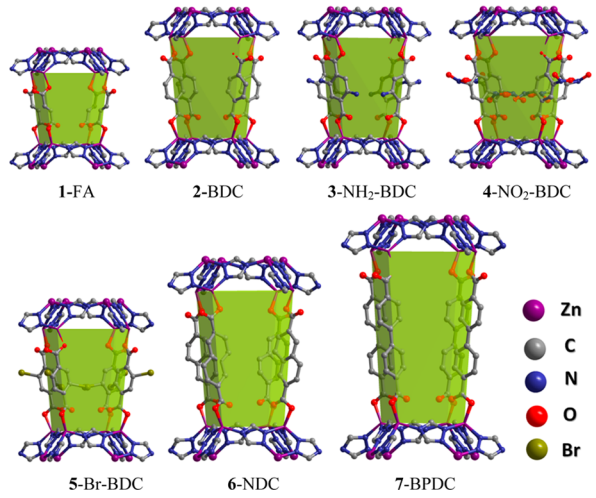

Figure 1. $\{[Zn_2(TRZ)_2]_8(dicarboxylate)_4\}$ building blocks in MOFs **1**–**7**.

Gas Adsorption. Pillar-layered Zn-triazolate-dicarboxylate MOFs **1**–**7** possess intersecting channels viewed along the *a*-, *b*-, or *c*-directions. PLATON calculations show that their guest-accessible volumes are 50.8%, 49.1%, 44.4%, 42.5%, 41.76%, 47.6%, and 51.4%, respectively. Furthermore, the TGA results show that these 3D pillar-layered frameworks are stable up to

DOI: 10.1021/acs.inorgchem.5b01611
Inorg. Chem. 2015, 54, 9862–9868

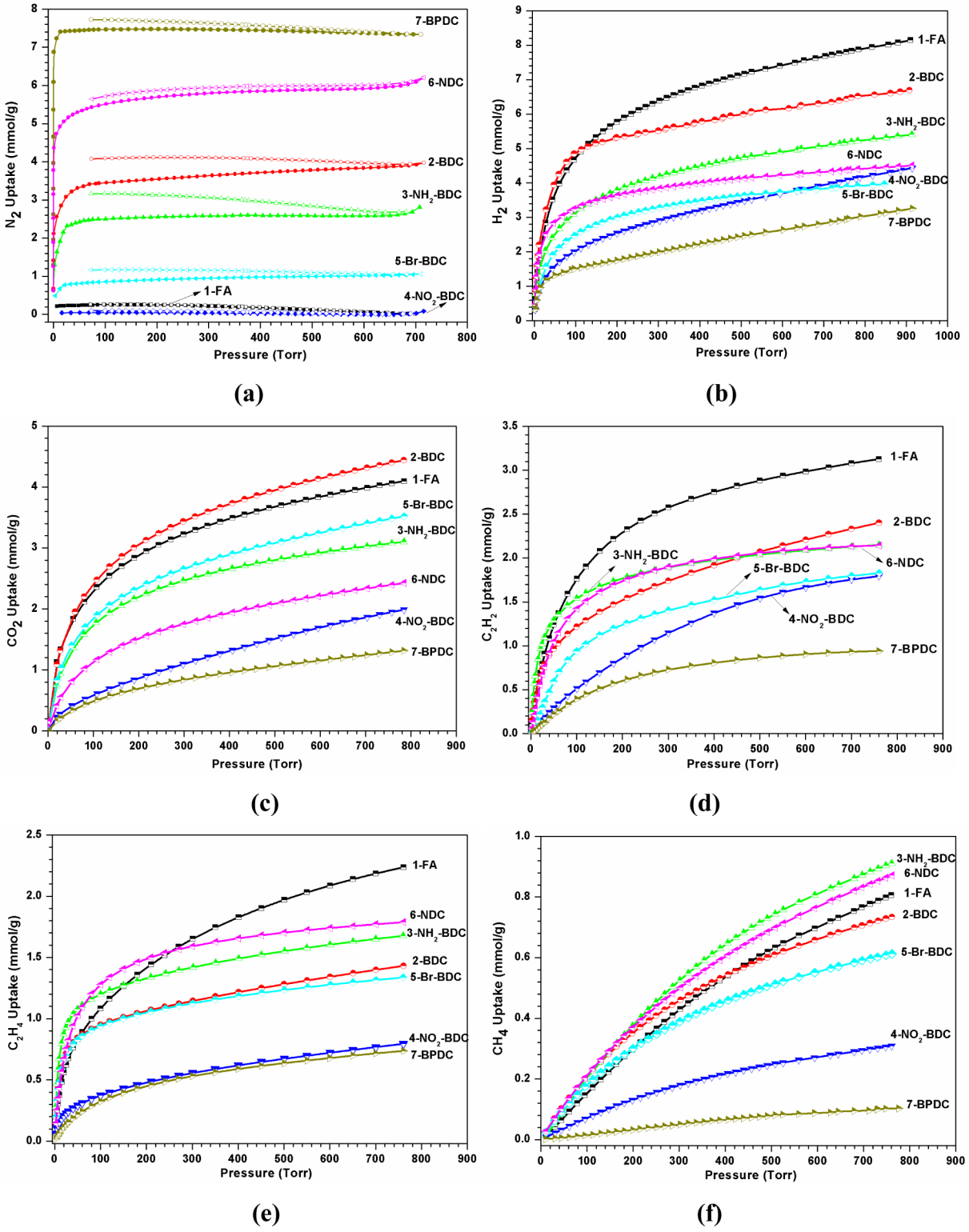

Figure 2. Adsorption isotherms of N_2 (a) and H_2 (b) at 77 K, CO_2 (c), C_2H_2 (d), C_2H_4 (e), and CH_4 (f) at 273 K for MOFs **1**–**7**.

about 300 °C for **1** and 380 °C for **2**–**7** (Figure S7). The weight losses (ca. 20%) from room temperature to about 200 °C should be attributed to the decomposition of entrapped solvent. Such high porosity and thermal stability render them suitable candidates for gas sorption applications. The N_2 sorption isotherms at 77 K (Figure 2a) indicate negligible uptakes for MOFs **1**-FA and **4**-NO_2-BDC, but a typical type I sorption behavior for MOFs **2**, **3**, and **5**–**7**, characteristic of microporous materials with a saturated sorption amount of N_2 of 3.98 mmol/g (**2**-BDC), 2.81 mmol/g (**3**-NH_2-BDC), 1.05 mmol/g (**5**-Br-BDC), 6.20 mmol/g (**6**-NDC), and 7.34 mmol/g (**7**-BPDC), respectively (Tables 1 and S5). The BET and Langmuir surface areas are 226.7 and 356.3 cm^3/g for **2**, 162.6 and 254.5 cm^3/g for **3**, 59.6 and 95.3 cm^3/g for **5**, 365.1 and

DOI: 10.1021/acs.inorgchem.5b01611
Inorg. Chem. 2015, 54, 9862–9868

Table 1. Gas Adsorption Data for Pillar-Layered MOFs 1−7

MOFs	N_2 (mmol/g)	H_2 (mmol/g)	CO_2 (mmol/g)		C_2H_2 (mmol/g)		C_2H_4 (mmol/g)		CH_4 (mmol/g)		IAST selectivity (50−50)		
	77 K, 1 atm	77 K, 1 atm	273 K, 1 atm	298 K, 1 atm	273 K, 1 atm	298 K, 1 atm	273 K, 1 atm	298 K, 1 atm	273 K, 1 atm	298 K, 1 atm	CO_2/CH_4	C_2H_2/CH_4	C_2H_4/CH_4
1-FA	0.02	7.84	4.06	3.55	3.13	2.07	2.24	1.54	0.81	0.43	78	36	38
2-BDC	3.98	6.48	4.40	2.46	2.40	1.76	1.43	1.18	0.73	0.50	52	30	37
3-NH_2-BDC	2.81	5.20	3.08	2.02	2.15	1.68	1.68	1.34	0.91	0.69	37	60	65
4-NO_2-BDC	0.03	4.09	1.95	0.95	1.79	1.05	0.80	0.47	0.31	0.14	35	4	84
5-Br-BDC	1.05	3.90	3.48	1.28	1.83	1.25	1.34	0.95	0.62	0.45	26	5	45
6-NDC	6.20	4.38	2.40	1.50	2.14	1.67	1.79	1.46	0.87	0.47	24	39	25
7-BPDC	7.34	2.97	1.29	0.76	0.94	0.18	0.74	0.23	0.10	0.03	62	120	189

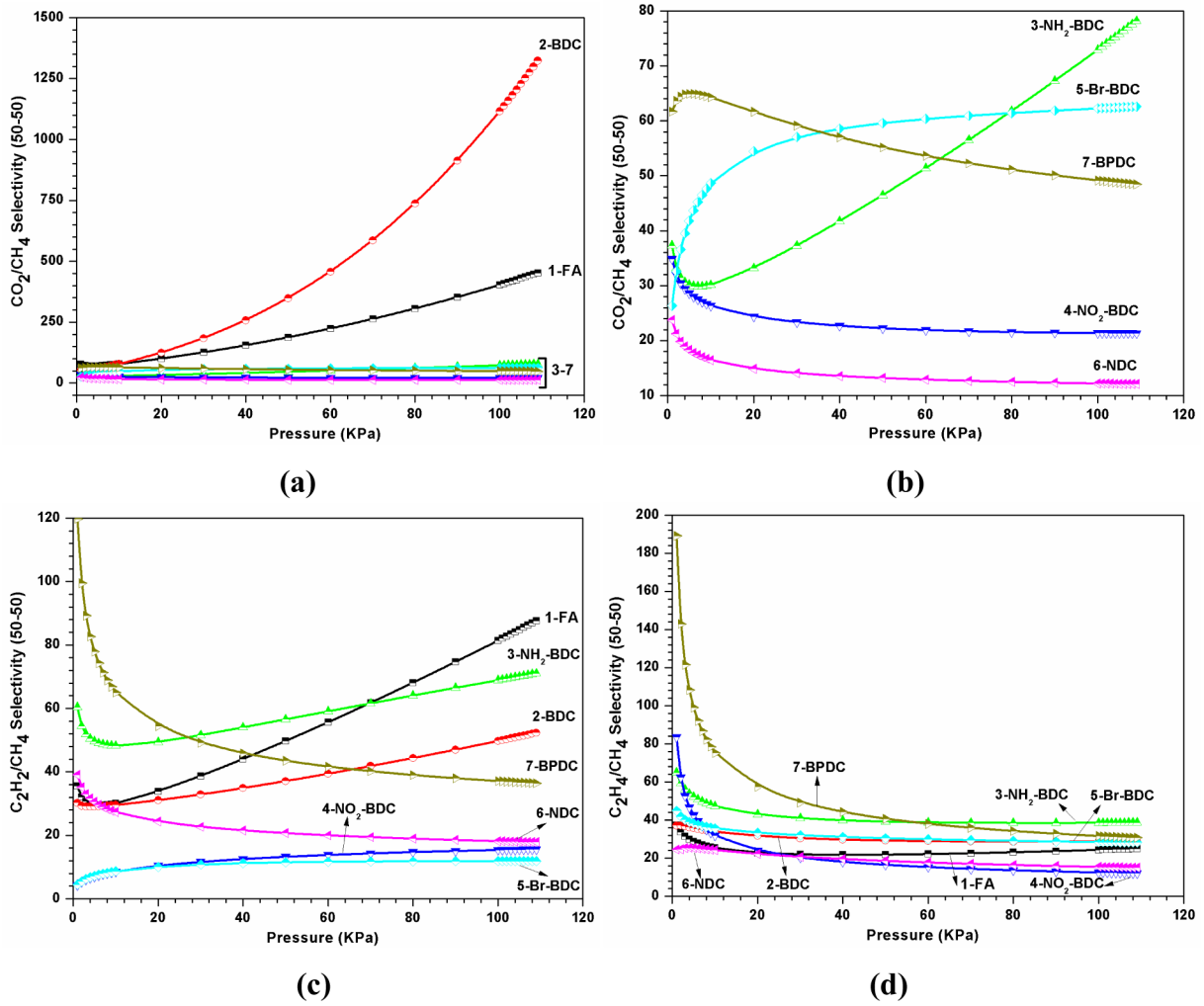

Figure 3. Adsorption selectivity predicted by IAST of MOFs **1**−**7** for CO_2 (50%)/CH_4 (50%) (a and b), C_2H_2 (50%)/CH_4 (50%) (c), and C_2H_4 (50%)/CH_4 (50%) (d) at 273 K.

574.9 cm^3/g for **6**, and 470.8 and 730.3 cm^3/g for **7** (Tables 1 and S5). Clearly, the surface areas gradually increase with the elongation of pillars (**1**-FA → **2**-BDC → **6**-NDC → 7-BPDC), and decrease with the group bulkiness from pillars (**2**-BDC → **3**-NH_2-BDC → **5**-Br-BDC → **4**-NO_2-BDC). The presence of the shortest FA pillar in **1** and the largest $-NO_2$ groups in **4** both led to negligible surface areas. Overall, the porosity of these pillar-layered structures is well tuned by the packing of the pillaring dicarboxylates within the interlamellar spaces. The H_2 sorption isotherms further prove this point (Figures 2b and S8). The similar pillar-layered MOF with oxalate bridges showed no H_2 uptakes at 77 K,[13] while compounds **1**−**7** exhibit remarkable H_2 adsorption. At 77 K and 1 atm, the H_2 uptakes reach 175.6 $cm^3\ g^{-1}$ (1.6 wt %) for **1**-FA, 145.2 $cm^3\ g^{-1}$ (1.3 wt %) for **2**-BDC, 116.5 $cm^3\ g^{-1}$ (1.1 wt %) for **3**-NH_2-BDC, 91.6 $cm^3\ g^{-1}$ (0.82 wt %) for **4**-NO_2-BDC, 87.4 $cm^3\ g^{-1}$ (0.78 wt %) for **5**-Br-BDC, 98.1 $cm^3\ g^{-1}$ (0.88 wt %) for **6**-NDC, and 66.5 $cm^3\ g^{-1}$ (0.59 wt %) for 7-BPDC (Tables 1 and S5). Considering the low surface area of these pillar-layered MOFs, their relatively high H_2 uptakes are notable. Specially, the H_2 adsorption of compound **1** is comparable to many well-known frameworks such as MOF-5[24] and ZIF-8,[25] which

DOI: 10.1021/acs.inorgchem.5b01611
Inorg. Chem. 2015, 54, 9862−9868

surpasses the values of all reported similar pillared-layer frameworks under the same temperature and pressure.[13−15]

The permanent porosity for Zn-triazolate-dicarboxylate frameworks encouraged us to examine their potential application in separating CO_2 from CH_4. The low-pressure CO_2 adsorption−desorption isotherms were measured at 273 and 298 K. As shown in Figure 2c, the CO_2 uptakes are 4.06 mmol/g (90.9 $cm^3\ g^{-1}$) for **1**-FA, 4.40 mmol/g (98.6 $cm^3\ g^{-1}$) for **2**-BDC, 3.08 $cm^3\ g^{-1}$ (69.0 $cm^3\ g^{-1}$) for **3**-NH_2-BDC, 1.95 (43.7 $cm^3\ g^{-1}$) for **4**-NO_2-BDC, 3.48 (78.0 $cm^3\ g^{-1}$) for **5**-Br-BDC, 2.40 mmol/g (53.8 $cm^3\ g^{-1}$) for **6**-NDC, and 1.29 mmol/g (28.9 $cm^3\ g^{-1}$) for **7**-BPDC at 273 K (Tables 1 and S5). The CO_2 uptake of compound **2** outperforms all of the values of similar metal-triazolate-dicarboxylate pillar-layered MOFs, even though most of them are decorated with amino groups.[13−15] At 298 K, MOF **1** exhibits the highest CO_2 uptake of 3.55 mmol/g (79.5 $cm^3\ g^{-1}$), and **7** shows the lowest value of 0.76 mmol/g (17.0 $cm^3\ g^{-1}$). Also, the 2.46 mmol/g (55.1 $cm^3\ g^{-1}$) CO_2 uptake of compound **2** surpasses the value (39.4 $cm^3\ g^{-1}$, 298 K and 1 atm) of iso-MOF [Zn(atz) $(BDC)_{0.5}$] with the same BDC pillars and 3-amino-1,2,4-triazole reported by Wang et al.[12g] Clearly, the explanation of the enhanced CO_2 uptakes of these Zn-triazolate-dicarboxylate pillar-layered MOFs[13−15] using the presence of amino groups is debatable. Other factors such as the synergistic effect of pore size and functionality may play a greater role.

It should be pointed out that our direct activation can greatly enhance CO_2 uptake (comparable to those made through CH_2Cl_2 solvent exchange[12h]) without simultaneously increasing N_2 uptake (in the literature,[12h] a concurrent increase in N_2 uptake was also observed). Thus, our study led to a dramatic increase in CO_2/N_2 selectivity (better than that activated through CH_2Cl_2 exchange). To my knowledge, this is the first demonstration that the sample activation can be employed to dramatically improve CO_2/N_2 selectivity.

C_2H_2 and C_2H_4 gas are selected in this work to evaluate the C2 hydrocarbons over CH_4 separation ability of these pillar-layered MOFs. At 273 K and 1 atm, the C_2H_2 and C_2H_4 uptakes (Figure 2d and e) are 3.13 and 2.24 mmol/g for **1**-FA, 2.40 and 1.43 mmol/g for **2**-BDC, 2.15 and 1.68 mmol/g for **3**-NH_2BDC, 1.79 and 0.80 mmol/g for **4**-NO_2-BDC, 1.83 and 1.34 mmol/g for **5**-Br-BDC, 2.14 and 1.46 mmol/g for **6**-NDC, and 0.94 and 0.74 mmol/g for **7**-BPDC (Tables 1 and S5). At 298 K and 1 atm, compound **1** shows the highest C_2H_2 uptake of 2.07 and 1.54 mmol/g (Figure S9). Although the C_2H_2 and C_2H_4 gas adsorption capacities of these pillar-layered MOFs are not very impressive, their accessible starting materials and easily handled situations still make them promising for C2 hydrocarbons over CH_4 separation applications. The CH_4 uptake capacities (Figure 2f) of MOFs **1**−**7** are 0.81 mmol/g (18.1 $cm^3\ g^{-1}$), 0.73 mmol/g (16.4 $cm^3\ g^{-1}$), 0.91 mmol/g (20.4 $cm^3\ g^{-1}$), 0.31 mmol/g (6.9 $cm^3\ g^{-1}$), 0.62 mmol/g (13.9 $cm^3\ g^{-1}$), 0.87 mmol/g (19.5 $cm^3\ g^{-1}$), and 0.10 mmol/g (2.2 $cm^3\ g^{-1}$) at 273 and 1 atm (Tables 1 and S5). The significantly lower CH_4 uptake values should be due to the weak interaction between CH_4 molecules and the frameworks of these pillar-layered MOFs with narrow cross pores.

CO_2/CH_4 and C2 Hydrocarbons/CH_4 Selectivity. The above-mentioned isothermal adsorption results indicate that MOFs **1**−**7** can selectively adsorb CO_2 and C2 hydrocarbons (C_2H_2 and C_2H_4) over CH_4. To predict CO_2−CH_4, C_2H_2−CH_4, and C_2H_4−CH_4 binary mixture selectivity, an ideal adsorbed solution theory (IAST) calculation based on a dual-site Langmuir−Freundlich (DSLF) simulation was employed on the basis of the single-component CO_2, C_2H_2, C_2H_4, and CH_4 adsorption isotherms.[26] Figure 3a and b shows the adsorption selectivity of MOFs **1**−**7** for CO_2 (50%) and CH_4 (50%) at 273 K. The CO_2/CH_4 selectivity values are estimated to be 78, 52, 37, 35, 26, 24, and 62 for **1**−**7**, respectively, which are significantly higher than the values of those reported for other Zn-triazolate-dicarboxylate pillar-layered MOFs[13−15] and are comparable to those of MOFs with the highest selectivity reported in the literature.[3] Figure 3c and d shows the predicted mixture adsorption selectivity of **1**−**7** for C_2H_2/CH_4 (50:50) and C_2H_4/CH_4 (50:50) at 273 K. The C_2H_2/CH_4 and C_2H_4/CH_4 selectivity values are estimated to be 36 and 38 for **1**, 30 and 37 for **2**, 60 and 65 for **3**, 4 and 84 for **4**, 5 and 45 for **5**, 39 and 25 for **6**, and 120 and 189 for **7** (Tables 1 and S5). These values are considered of very high selectivity among the limited MOFs investigated so far for separations of the C2 hydrocarbons (C_2H_2, C_2H_4, or C_2H_6) over CH_4.[6] Overall, the tunable CO_2 and C2 hydrocarbons selectivity over CH_4 for MOFs **1**−**7** could be due to the synergistic effect of multiple functional groups and their narrow cross pores. Moreover, the more hydrophobic pore nature enforces the pillar-layered frameworks' stability under humid environments, which is favorable for their potential application in the separation of CO_2 and C2 hydrocarbons from CH_4.

CONCLUSIONS

By employment of typical Zn-triazolate layer and linear ditopic carboxylate ligands, we present a systematic design of pore size and functionality in Zn-triazolate-dicarboxylate pillar-layered MOFs. The substituent groups and longer pillars do not promote CO_2 adsorption capacity and CO_2/CH_4 separation performance; however, longer pillars can increase the C_2H_2/CH_4 and C_2H_4/CH_4 selectivity. Overall, the narrow intersecting channels together with the functional groups effectively tune the CO_2 and C2 hydrocarbons uptakes and reduce the affinity with CH_4, which demonstrate the potential of these pillar-layered MOFs as promising candidate materials for separation from natural gas and fuel gases. The synergistic effect demonstrated herein by tuning functional groups and controlling the pore size simultaneously may be a promising strategy to enhance gas adsorption capacity and separation performance of MOFs.

ASSOCIATED CONTENT

Supporting Information

The Supporting Information is available free of charge on the ACS Publications website at DOI: 10.1021/acs.inorgchem.5b01611.

Powder X-ray diffraction patterns, TGA curves, FT-IR spectra, gas adsorption isotherms, additional crystal structure figures, crystallographic table, and CIF files for MOFs **1**−**7** (PDF)

X-ray data for compound **1** (CIF)

AUTHOR INFORMATION

Corresponding Authors

*E-mail: xianhui.bu@csulb.edu.

*E-mail: pingyun.feng@ucr.edu.

Notes

The authors declare no competing financial interest.

DOI: 10.1021/acs.inorgchem.5b01611
Inorg. Chem. 2015, 54, 9862−9868

■ ACKNOWLEDGMENTS

The work is supported by the U.S. Department of Energy, Office of Basic Energy Sciences, Materials Sciences and Engineering Division, under award no. DE-FG02-13ER46972.

■ REFERENCES

(1) Choudhary, V. R.; Mayadevi, S. *Sep. Sci. Technol.* **1993**, *28*, 2197−2209.
(2) Cavenati, S.; Grande, C. A.; Rodrigues, A. E. *Energy Fuels* **2006**, *20*, 2648−2659.
(3) Li, J. R.; Sculley, J.; Zhou, H. C. *Chem. Rev.* **2012**, *112*, 869−932.
(4) (a) Zhang, Z.; Yao, Z.-Z.; Xiang, S.; Chen, B. *Energy Environ. Sci.* **2014**, *7*, 2868−2899. (b) Sumida, K.; Rogow, D. L.; Mason, J. A.; McDonald, T. M.; Bloch, E. D.; Herm, Z. R.; Bae, T.-H.; Long, J. R. *Chem. Rev.* **2012**, *112*, 724−781. (c) Li, J. R.; Ma, Y. G.; McCarthy, M. C.; Sculley, J.; Yu, J. M.; Jeong, H. K.; Balbuena, P. B.; Zhou, H. C. *Coord. Chem. Rev.* **2011**, *255*, 1791−1823. (d) D'Alessandro, D. M.; Smit, B.; Long, J. R. *Angew. Chem., Int. Ed.* **2010**, *49*, 6058−6082. (e) Kitagawa, S.; Kitaura, R.; Noro, S. *Angew. Chem., Int. Ed.* **2004**, *43*, 2334−2375. (f) Yi, F. Y.; Jiang, H. L.; Sun, Z. M. *Chem. Commun.* **2015**, *51*, 8446−8449. (g) Zhou, Y. X.; Chen, Y. Z.; Cao, L.; Lu, J.; Jiang, H. L. *Chem. Commun.* **2015**, *51*, 8292−8295. (h) Li, S. L.; Zhang, F. Q.; Zhang, X. M. *Chem. Commun.* **2015**, *51*, 8062−8065. (i) Liu, J.; Qu, M.; Clérac, R.; Zhang, X. M. *Chem. Commun.* **2015**, *51*, 7356−7359.
(5) (a) Bae, Y. S.; Lee, C. Y.; Kim, K. C.; Farha, O. K.; Nickias, P.; Hupp, J. T.; Nguyen, S. T.; Snurr, R. Q. *Angew. Chem., Int. Ed.* **2012**, *51*, 1857−1860. (b) Lee, J. Y.; Pan, L.; Huang, X. Y.; Emge, T. J.; Li, J. *Adv. Funct. Mater.* **2011**, *21*, 993−998. (c) Lan, Y. Q.; Jiang, H. L.; Li, S. L.; Xu, Q. *Adv. Mater.* **2011**, *23*, 5015−5020. (d) Holst, J. R.; Cooper, A. I. *Adv. Mater.* **2010**, *22*, 5212−5216. (e) Furukawa, H.; Ko, N.; Go, Y. B.; Aratani, N.; Choi, S. B.; Choi, E.; Yazaydin, A. O.; Snurr, R. Q.; O'Keeffe, M.; Kim, J.; Yaghi, O. M. *Science* **2010**, *329*, 424−428. (f) Ma, S. Q.; Sun, D. F.; Simmons, J. M.; Collier, C. D.; Yuan, D. Q.; Zhou, H. C. *J. Am. Chem. Soc.* **2008**, *130*, 1012−1016. (g) Férey, G.; Mellot-Draznieks, C.; Serre, C.; Millange, F.; Dutour, J.; Surble, S.; Margiolaki, I. *Science* **2005**, *309*, 2040−2042. (h) Li, J.; Chen, Y.; Tang, Y.; Li, S.; Dong, H.; Li, K.; Han, M.; Lan, Y. Q.; Bao, J.; Dai, Z. *J. Mater. Chem. A* **2014**, *2*, 6316−6319. (i) Bao, S. J.; Krishna, R.; He, Y.; Qin, J. S.; Su, Z. M.; Li, S. L.; Xie, W.; Du, D. Y.; He, W. W.; Zhang, S. R.; Lan, Y. Q. *J. Mater. Chem. A* **2015**, *3*, 7361−7367. (j) Zhao, X.; Liu, F.; Zhang, L.; Sun, D.; Wang, R.; Ju, Z.; Yuan, D. Q.; Sun, D. *Chem. - Eur. J.* **2014**, *20*, 649−652. (k) Ding, H.; Yang, Y.; Li, B.; Pan, F.; Zhu, G.; Zeller, M.; Yuan, D.; Wang, C. *Chem. Commun.* **2015**, *51*, 1976−1979.
(6) (a) Duan, J.; Higuchi, M.; Horike, S.; Foo, M. L.; Rao, K. P.; Inubushi, Y.; Fukushima, T.; Kitagawa, S. *Adv. Funct. Mater.* **2013**, *23*, 3525−3530. (b) He, Y. B.; Zhang, Z. J.; Xiang, S. C.; Fronczek, F. R.; Krishna, R.; Chen, B. L. *Chem. - Eur. J.* **2012**, *18*, 613−619. (c) Horike, S.; Kishida, K.; Watanabe, Y.; Inubushi, Y.; Umeyama, D.; Sugimoto, M.; Fukushima, T.; Inukai, M.; Kitagawa, S. *J. Am. Chem. Soc.* **2012**, *134*, 9852−9855.
(7) (a) Zhang, Z.; Zhao, Y.; Gong, Q.; Li, J. *Chem. Commun.* **2013**, *49*, 653−661. (b) Xiang, S.; He, Y.; Zhang, Z.; Wu, H.; Zhou, W.; Krishna, R.; Chen, B. *Nat. Commun.* **2012**, *3*, 954. (c) Zhang, Z.; Xiang, S.; Chen, Y.-S.; Ma, S.; Lee, Y.; Phely-Bobin, T.; Chen, B. *Inorg. Chem.* **2010**, *49*, 8444−8448. (d) Frost, H.; Duren, T.; Snurr, R. Q. *J. Phys. Chem. B* **2006**, *110*, 9565−9570.
(8) (a) Zheng, B.; Yang, Z.; Bai, J.; Li, Y.; Li, S. *Chem. Commun.* **2012**, *48*, 7025−7027. (b) Lin, Q.; Wu, T.; Zheng, S.; Bu, X.; Feng, P. *J. Am. Chem. Soc.* **2012**, *134*, 784−787. (c) Liu, H.; Zhao, Y.; Zhang, Z.; Nijem, N.; Chabal, Y. J.; Zeng, H.; Li, J. *Adv. Funct. Mater.* **2011**, *21*, 4754−4762. (d) Zheng, B.; Bai, J.; Duan, J.; Wojtas, L.; Zaworotko, M. J. *J. Am. Chem. Soc.* **2011**, *133*, 748−751. (e) Pachfule, P.; Chen, Y.; Jiang, J.; Banerjee, R. *J. Mater. Chem.* **2011**, *21*, 17737−17745.
(9) (a) Zheng, S.-T.; Zhao, X.; Lau, S.; Fuhr, A.; Feng, P.; Bu, X. *J. Am. Chem. Soc.* **2013**, *135*, 10270−10273. (b) Britt, D.; Furukawa, H.; Wang, B.; Glover, T. G.; Yaghi, O. M. *Proc. Natl. Acad. Sci. U. S. A.* **2009**, *106*, 20637−20640. (c) Dietzel, P. D. C.; Besikiotis, V.; Blom, R. *J. Mater. Chem.* **2009**, *19*, 7362−7370. (d) Caskey, S. R.; Wong-Foy, A. G.; Matzger, A. J. *J. Am. Chem. Soc.* **2008**, *130*, 10870−10871.
(10) (a) Farha, O. K.; Bae, Y.-S.; Hauser, B. G.; Spokoyny, A. M.; Snurr, R. Q.; Mirkin, C. A.; Hupp, J. T. *Chem. Commun.* **2010**, *46*, 1056−1058. (b) Zheng, S.-T.; Bu, J. T.; Li, Y.; Wu, T.; Zuo, F.; Feng, P.; Bu, X. *J. Am. Chem. Soc.* **2010**, *132*, 17062−17064.
(11) Zhang, J. P.; Chen, X. M. *Chem. Commun.* **2006**, 1689−1699.
(12) (a) Park, H.; Moureau, D. M.; Parise, J. B. *Chem. Mater.* **2006**, *18*, 525−531. (b) Park, H.; Britten, J. F.; Mueller, U.; Lee, J. Y.; Li, J.; Parise, J. B. *Chem. Mater.* **2007**, *19*, 1302−1308. (c) Park, H.; Krigsfeld, G.; Parise, J. B. *Cryst. Growth Des.* **2007**, *7*, 736−740. (d) Lin, Y.; Zhang, Y.; Zhang, J. P.; Chen, X. M. *Cryst. Growth Des.* **2008**, *8*, 3673−3679. (e) Ren, H.; Song, T.; Xu, J.; Jing, S.; Yu, Y.; Zhang, P.; Zhang, L. *Cryst. Growth Des.* **2009**, *9*, 105−112. (f) Luo, M.; Yuan, Z.; Xu, W.; Luo, F.; Li, J.; Zhu, Y.; Feng, X.; Liu, S. *Dalton Trans.* **2013**, *42*, 13802−13805. (g) Liu, B.; Zhao, R.; Yang, G.; Hou, L.; Wang, Y. Y.; Shi, Q. Z. *CrystEngComm* **2013**, *15*, 2057−2060. (h) Hu, X.-L.; Liu, F.-H.; Wang, H.-N.; Qin, C.; Sun, C.-Y.; Su, Z.-M.; Liu, F.-C. *J. Mater. Chem. A* **2014**, *2*, 14827−14834. (i) Yang, E.-C.; Liu, T.-Y.; Wang, Q.; Zhao, X.-J. *Inorg. Chem. Commun.* **2011**, *14*, 285−287. (j) Gao, J.; Wang, N.; Xiang, X.; Chen, C.; Xie, W.; Ran, X.; Long, Y.; Yue, S.; Liu, Y. *CrystEngComm* **2013**, *15*, 3261−3270. (k) Huang, C.; Ji, F.; Liu, L.; Li, N.; Li, H.; Wu, J.; Hou, H.; Fan, Y. *CrystEngComm* **2014**, *16*, 2615−2625. (l) Zhang, Y.; Chen, S.; Gao, S. *Z. Anorg. Allg. Chem.* **2009**, *635*, 537−543.
(13) (a) Vaidhyanathan, R.; Iremonger, S. S.; Dawson, K. W.; Shimizu, G. K. H. *Chem. Commun.* **2009**, 5230−5232. (b) Vaidhyanathan, R.; Iremonger, S. S.; Shimizu, G. K. H.; Boyd, P. G.; Alavi, S.; Woo, T. K. *Science* **2010**, *330*, 650−653.
(14) Chen, K. J.; Lin, R. B.; Liao, P. Q.; He, C. T.; Lin, J. B.; Xue, W.; Zhang, Y. B.; Zhang, J. P.; Chen, X. M. *Cryst. Growth Des.* **2013**, *13*, 2118−2123.
(15) Liu, B.; Shi, J.; Yue, K.; Li, D.; Wang, Y. *Cryst. Growth Des.* **2014**, *14*, 2003−2008.
(16) Zhai, Q. G.; Lin, Q.; Wu, T.; Wang, L.; Zheng, S. T.; Bu, X.; Feng, P. *Chem. Mater.* **2012**, *24*, 2624−2626.
(17) Sheldrick, G. M. *Acta Crystallogr., Sect. A: Found. Crystallogr.* **2008**, *64*, 112−122.
(18) Spek, A. L. *J. Appl. Crystallogr.* **2003**, *36*, 7−13.
(19) Bae, Y. S.; Mulfort, K. L.; Frost, H.; Ryan, P.; Punnathanam, S.; Broadbelt, L. J.; Hupp, J. T.; Snurr, R. Q. *Langmuir* **2008**, *24*, 8592−8598.
(20) Cessford, N. F.; Seaton, N. A.; Duren, T. *Ind. Eng. Chem. Res.* **2012**, *51*, 4911−4921.
(21) Babarao, R.; Hu, Z. Q.; Jiang, J. W.; Chempath, S.; Sandler, S. I. *Langmuir* **2007**, *23*, 659−666.
(22) Goetz, V.; Pupier, O.; Guillot, A. *Adsorption* **2006**, *12*, 55−63.
(23) Zhang, J. P.; Lin, Y. Y.; Huang, X. C.; Chen, X. M. *J. Am. Chem. Soc.* **2005**, *127*, 5495−5506.
(24) Li, H.; Eddaoudi, M.; O'Keeffe, M.; Yaghi, O. M. *Nature* **1999**, *402*, 276−279.
(25) Banerjee, R.; Phan, A.; Wang, B.; Knobler, C.; Furukawa, H.; O'Keeffe, M.; Yaghi, O. M. *Science* **2008**, *319*, 939−943.
(26) Xiong, S.; Gong, Y.; Wang, H.; Wang, H.; Liu, Q.; Gu, M.; Wang, X.; Chen, B.; Wang, Z. *Chem. Commun.* **2014**, *50*, 12101−12104.

DOI: 10.1021/acs.inorgchem.5b01611
Inorg. Chem. 2015, 54, 9862−9868